Original Research Article

Understanding climate modes' impact on the Indian Ocean decadal upwelling variability

Xiaolin Zhang

Department of Earth and Planetary Sciences, Kyushu University, 744 Motooka, Nishiku, Fukuota 819-0395, Japan; xz12j@my.fsu.edu

Abstract: This study explores the spatial pattern and climate modes' impact on the Indian Ocean decadal upwelling variability by using observational dataset, Static Linear Regression Model (SLM) and Bayesian Dynamic Linear Model (BDLM). Our analysis shows that the Indian Ocean decadal upwellings averaged in the Eastern and Western Indian Ocean (EIO and WIO) regions are positively correlated. Moreover, the BDLM that represents the temporal modulations of the El Niño and Southern Ocean (ENSO) and Indian Ocean Dipole (IOD) impacts, reproduces the time series of the EIO and WIO upwellings more realistically than a conventional SLM does. BDLM simulations further suggest that in both EIO and WIO, IOD is more important than ENSO impact. The time-varying regression coefficients in BDLM indicate that the observed shift of the IOD impact on the EIO upwelling around 1985 is mainly associated with the changes of alongshore wind stress forcing and the sensitivity of the upper ocean temperature in the EIO through the surface warming tendency and the enhanced ocean stratification. This suggests that climate models need to consider the time-varying impact of different climate modes in order to simulate the Indian Ocean dynamics correctly.

Keywords: Indian Ocean; decadal upwelling variability; El Niño and Southern Oscillation; Indian Ocean Dipole; climate shift

1. Introduction

Intense seasonally reversing monsoon wind forcing prevails in the Indian Ocean, namely south easterly wind dominates in the southern Indian Ocean through the year, and north easterly wind blows along Somalia, Oman in January and reverses in July (see Figure 2 in the work of Han et al.[1]). The monsoonal winds locally force a seasonally reversing Somali Current. In both the eastern Indian Ocean (EIO) and the western Indian Ocean (WIO), seasonal and annual mean upwelling occurs (see Figure 1 in the work of Zhang and Han[2]), which is important to regional and global climate, for instance, Sea Surface Temperature anomaly along the eastern coast[3] and Indian Ocean monsoon. There are two main upwelling regions in the Indian Ocean, namely the Seychelles–Chagos thermocline ridge (SCTR)[4–8]) and the seasonally changed upwelling along the coastal area of EIO (**Figure 1c)**[9,10]. Upwellings in the Indian Ocean exhibit decadal variability; however, the spatial pattern of upwellings and the relationship between upwellings in the EIO and WIO regions are still unclear.

A few mechanisms are responsible for the formation of upwelling formation, such as the oceanic Rossby waves and local Ekman Pumping[11,12]. Previous works have also suggested that the interannual anomaly of depth of 20 ℃ isotherm (D20) in the WIO upwelling zone is primarily caused by Rossby waves driven by winds in the central and eastern Indian Ocean. A number of studies indicated the importance of Rossby waves over the southern Indian Ocean[2,13–26]. The Indonesian throughflow variations in this area are weak[27] but can also show significant contributions to the southeast Indian Ocean[12,28,29].

Received: 25 July 2023 Accepted: 16 August 2023 Available online: 10 October 2023

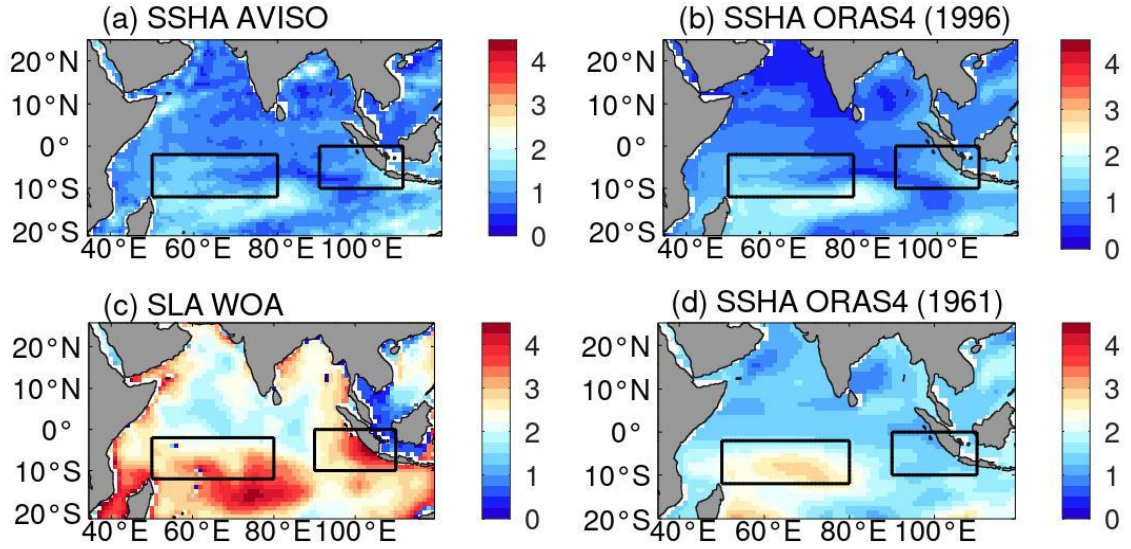

Figure 1. Standard deviation (STD) of decadal variability (annual mean + 7-year filter) of **(a)** SSHA (units: cm) based on AVISO SSHA from 1996 to 2013, **(b)** SSHA (referred to as ZOS) based on ORAS4 reanalysis from 1996 to 2013, **(c)** WOA13 upper 700 m thermosteric sea level anomaly (SLA; cm) for 1961–2012, and **(d)** SSHA based on ORAS4 reanalysis from 1961 to 2013.

The Indian Ocean Dipole (IOD) and the El Niño Southern Oscillation (ENSO) are two major climate modes that cause the Indian Ocean variability. Previous studies have tried to estimate the relative importance of the individual climate modes and have suggested that at interannual timescale, ENSO dominates the wind-driven Rossby waves south of 10° S whereas the IOD dominates north of 10° S[25,30–33]. On the other hand, Deepa et al.[28] suggest that larger sea level variability both north and south of 10° S during pure positive IOD compared to pure El Niño years, and the co-occurrence of IOD and ENSO significantly enhances the variability in magnitude. Murtugudde et al.[34] also indicated both the local and remote forcings contribute to the interannual anomaly of upwelling in the EIO[3,35]. In fact, Susanto et al.[9] suggested that ENSO plays a major role in the interannual variability of coastal upwelling along the Sumatra and Java coast, while other studies suggested that the IOD is more important than ENSO in causing the EIO upwelling[3,32,36]. Recently, by using Bayesian Dynamic Linear Ocean model, Zhang and Han[2] suggested that ENSO is more important than IOD to the interannual upwelling over the SCTR region, and they play a comparable role in the EIO and the impacts of ENSO on EIO upwelling are changing among ENSO diversities. Although plenty research has been done in terms of climate modes impact on interannual time scales, few studies have been done to understand the impact of ENSO and IOD on Indian Ocean decadal upwelling variability, especially the time-varying impact of ENSO and IOD. In this paper, we will firstly explore the spatial pattern of Indian Ocean decadal upwelling variability and the relationship between upwelling averaged in EIO and WIO boxed regions. By using an advanced statistical tool, BDLM, we will further explore the time-varying impact of ENSO and IOD on the Indian Ocean upwelling averaged in each boxed region and associated dynamics. Comparing to previous studies that are mostly based on a static linear regression model, our study will provide more realistic estimation of climate modes' impacts on the EIO and WIO upwellings.

The paper is organized as follows. A brief description of the data and approach are described in Section 2. Section 3 discusses the observed features of Indian Ocean decadal upwelling variability. Section 4 describes the relationship between the upwelling in the EIO and WIO and the contributions of IOD and ENSO. Section 5 explores the decadal shift of IOD impact on EIO as well as the underlying mechanisms responsible for these changes. Concluding remarks and further discussion are provided in Section 6.

2. Data approach

2.1. Datasets and climate modes

The depth of the thermocline, which is often represented by D20, is used for detecting upwelling. In this paper, D20 is calculated from the 1° × 1° monthly temperature data of European Centre for Medium-Range Weather Forecasts (ECMWF) Ocean Reanalysis System 4 (ORAS4) available for 1958–2016[37]. The 1° × 1° gridded sea surface temperature (SST) data from Hadley Centre Sea Ice and Sea Surface Temperature data set (HadISST)[38] available since 1870 is also used here. According to the one-and-a-half-layer model, a deeper (shallower) thermocline corresponds to a higher (lower) sea surface height (SSH), the 1° × 1° SSH anomaly (SSHA) dataset from ORAS4, and the 1/4° × 1/4° monthly SSHA from Archiving, Validation, and Interpretation of Satellite Oceanography (AVISO) data from 1993 to 2016 are also used as a proxy of upwelling. Moreover, the monthly upper 700 m thermosteric sea level data from World Ocean Atlas 2013 (WOA13)[39] from 1959 to 2015 is also analyzed. In this paper, we obtain monthly anomalies by removing the monthly climatologies and linear trends of each dataset for the periods of interest. The decadal variability is defined by estimating the annual mean with a seven-year running mean filter.

The 2.5° × 2.5° monthly wind stress for the period of National Centers for Environmental Prediction (NCEP)[40]; and the 2.5° × 2.5° monthly National Oceanic and Atmospheric Administration (NOAA) precipitation available for 1948–present[41,42] are also used to understand the processes that are associated with the impact of ENSO and IOD on WIO and EIO decadal upwelling variability.

Here we mainly focus on two major climate modes, namely ENSO and IOD. ENSO is defined by using the Niño3.4 index, which is the SST anomaly (SSTA) averaged in the (5° N–5° S, 170° W–120° W) region. The IOD is detected by the dipole mode index (DMI), defined as the SSTA difference between the western pole (10° S–10° N, 50° E–70° E) and eastern pole (10° S–0°, 90° E–110° E), following Saji et al.[43]. The Niño3.4 index and DMI from 1958 to 2016 indicate that there are 18 El Niño events and 10 positive IOD events (**Figure 1e**). Seven El Niño and positive IOD events co-occurred (i.e., 1963, 1972, 1982, 1994, 1997, 2006 and 2015).

2.2. The static linear model and Bayesian dynamic linear model

Following Zhang and Han[2], the conventional static linear regression model (SLM, $Y(t) = b_0 + b_1X_1 + \varepsilon_t$) is used to quantify the contribution of different climate modes on EIO and WIO upwellings. As described by Zhang and Han[2], here we used ENSO and IOD indices respectively as a single predictor (X_1). The response variable ($Y(t)$) represents upwelling time series (SSTA, SLA, SSHA) in each boxed region or at a gridded point. Since the regression coefficients (b_i) in SLM are time independent, and SLM can only measure the stationary influence of the predictor on the predictand. However, in reality, the relationship between the predictor and predictand is often changing with time[2,44–51]. A Bayesian dynamic linear model (BDLM, $Y(t) = b_0(t) + b_1(t)\ X_1(t) + \varepsilon(t)$) is further used to estimate the time-varying impact of each climate mode. More details on the SLM and BDLM can be found in various studies[49,52–54]. Also note here, that we used ENSO and IOD indices separately since they are correlated. In this way, our estimation represents the maximum amount of variance that might be attributed to ENSO and IOD[2,55].

3. Observed upwelling features

In order to see the spatial pattern of Indian Ocean upwelling decadal variability, we first plot the standard deviation (STD) of decadal upwelling based on AVISO SSHA (**Figure 1a**), ORAS4 SSHA (**Figure 1d**), and SLA from WOA (**Figure 1c**). Clearly, we can see large SSH fluctuations in the WIO (boxed by 50° E–80° E, 2° S–15° N, about 3 cm) and central Indian Ocean (about 2.5 cm). Large fluctuation also appears

along the coastal area of EIO and the eastern coast of Bay of Bengal (about 3 cm). **Figure 1b** is STD of ORAS4 SSHA from 1996 to 2013, which shows the similar pattern with AVISO SSHA (**Figure 1a**), suggesting that the ORAS4 dataset can capture the feature of satellite measurement. The satellite observation (**Figure 1a**) based on AVISO satellite measurement also shows large variability in the northern Indian Ocean coastal region, which may be caused by the freshwater flux forcing or eddy activities. Zhang and Mochizuki[55] suggest that the SSHA in the northwestern Indian Ocean is partly related to the Asian summer monsoon forcing. In order to see the relationship between upwellings in the EIO and WIO boxed region, we further calculated the correlation between these two-time series (**Figure 2**). We can see that the upwellings in the EIO and WIO are positively correlated, with a correlation of 0.52 for WOA SLA, 0.60 for ORAS4 SSHA, and 0.67 for HadISST (see **Figure 2b**,**c**,**d**). The correlation based on ORAS4 D20 is only 0.08, which may be due to the uncertainties of the dataset. **Figure 2e** and **f** are the standard deviations (STD) of each time series. The STD for D20A in the EIO is 1.85 m, in the WIO is 2.74 m, for WOA in the EIO is 1.21 cm, in the WIO is 0.93 cm, for ORAS4 SSHA is 1.22 cm in the EIO and 1.94 cm in the WIO, for HadISST is 0.08 ℃ in EIO and 0.05 ℃ in WIO. In the following section, we will try to estimate the climate mode contributions of EIO and WIO upwellings.

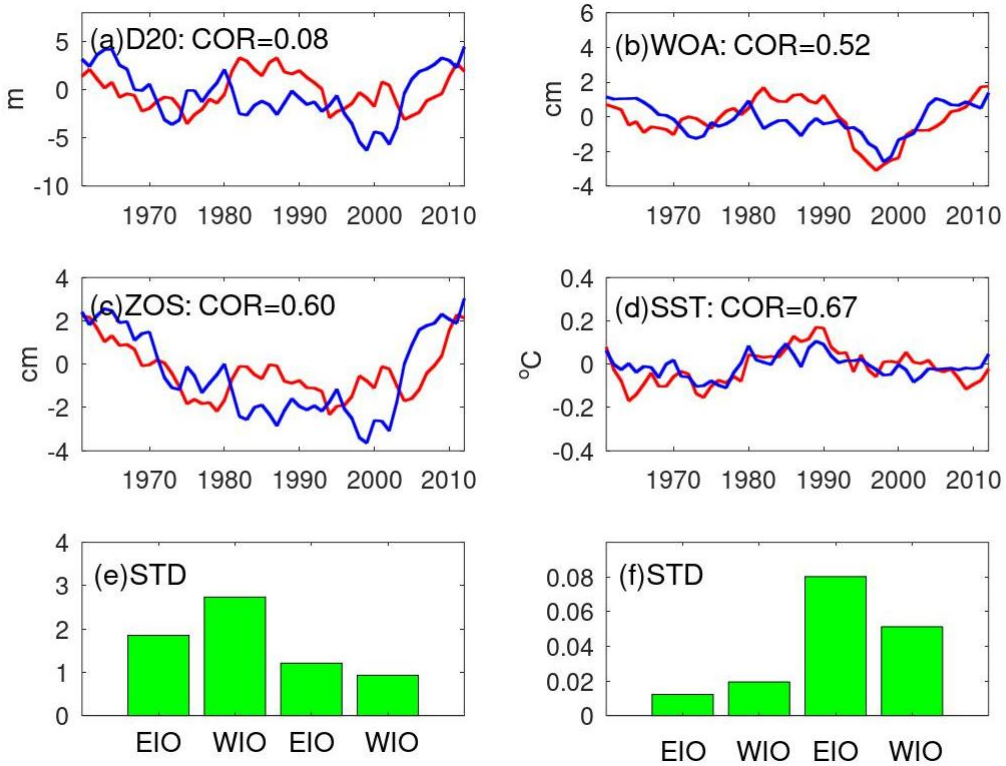

Figure 2. Time series of decadal variability of (annual mean + 7-year filter) **(a)** ORAS4 D20A, **(b)** WOA13 SLA, **(c)** ORAS4 SSHA, and **(d)** SSTA from HadISST averaged in the WIO (red line) and EIO (blue line) mean and seasonal upwelling zones (boxed regions of **Figure 1**). The correlation is shown in each panel. **(e)**–**(f)** Standard deviations of each time series.

4. Climate mode contributions to EIO and WIO upwellings

As mentioned earlier, ENSO and IOD are two major climate modes controlling upwellings in the IO. In this section, we will try to quantify the contribution of each climate mode in the two boxed regions. **Figure 3** shows the time series of Indian Ocean decadal upwelling in the EIO and WIO and the contribution of ENSO and IOD impact. We can see that the BDLM can simulate upwellings better than SLM, with a correlation of 0.34 (cor (SLM) = 0.27) for ENSO effect in the EIO, 0.39 (cor (SLM) = 0.18) in the WIO, 0.65 (cor (SLM) = 0.07) for IOD impact on EIO, and 0.72 (cor (SLM) = 0.19)) for WIO. Furthermore, we can see that IOD is

more important than ENSO for the upwellings in both EIO and WIO. The STD of observation for EIO is 1.8 cm, ENSO effect based on DLM is 0.6 cm, and IOD effect is 0.86 cm. The STD of observation for WIO is 2.4 cm, the ENSO effect based on DLM is 0.75 cm, and IOD effect is 0.94 cm.

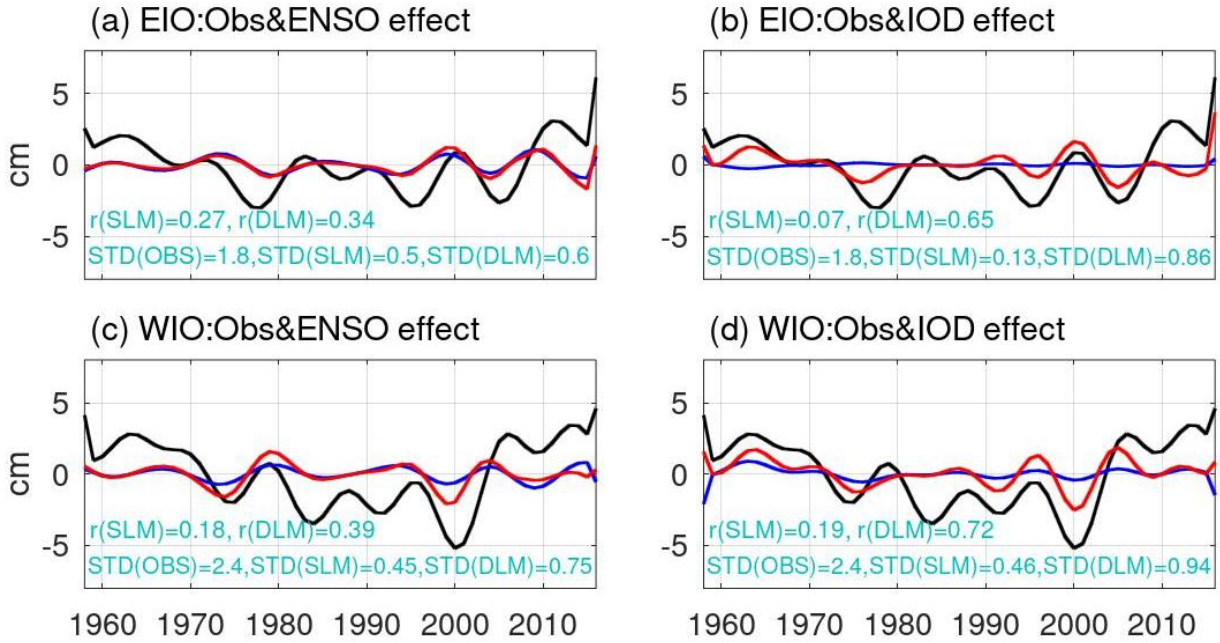

Figure 3. Time series of decadal ORAS4 SSHA (black line), SSHA explained by ENSO index (i.e., Niño 3.4 index) using conventional Static Linear Model (SLM; blue line) and Bayesian dynamical linear model (BDLM; red line), for **(a)** EIO box, **(c)** WIO box, shown in **Figure 1**. Panels **(b)** and **(d)** are the same as panels **(a)** and **(c)**, respectively, but for SSHA explained by the IOD index (i.e., DMI). Specifically, the blue and red lines are the b_1X_1 terms of SLM and BDLM, respectively, with X_1 being Niño3.4 index for **(a)**, **(c)** and DMI for **(b)**, **(d)**. The correlations between AVISO observed SSHA and modeled SSHA using SLM (BDLM) and the standard deviations of each time series are also shown at the bottom of each panel.

Figure 4 is the regression of SSHA and precipitation onto the ENSO and IOD indices. During positive IOD events, the weakened convection (e.g., reduced precipitation and enhanced outgoing longwave radiation at the top of the atmosphere) in the eastern basin and the enhanced convection in the western basin, will drive easterly wind stress anomalies in the equatorial basin and alongshore winds along Sumatra and Java coast, which will further increase coastal and equatorial upwelling in the EIO and reduce the upwelling in the WIO. The upwelling signals can also propagate into the Bay of Bengal, and reduce the sea level over the eastern and northern Bay. Meanwhile, the easterly wind anomalies induce negative Ekman Pumping velocity in the eastern basin, which forces positive SSHA. The positive SSHA can propagate westward, reducing upwelling in the WIO.

Overall, our analysis suggests that the BDLM simulates observed upwellings in the WIO and EIO better than SLM and in both EIO and WIO, and IOD is more important than ENSO effect. Since the BDLM can also simulate the time-varying impact of climate modes on upwelling, in the following section, we try to explain the possible underlying processes that can contribute to the shift of climate modes' impact on IO upwelling.

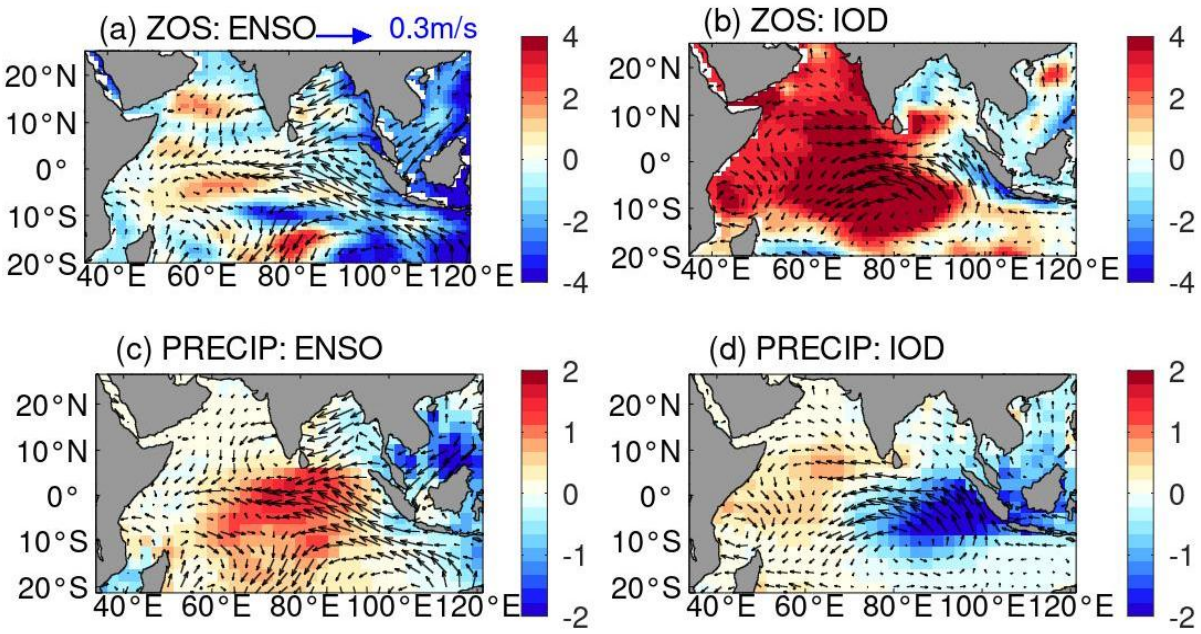

Figure 4. The regression of atmospheric and oceanic variability onto the ENSO index (annual mean + 7-year filter) from 1961 to 2013 in the results of SLM. Color shades and vectors show **(a)** SSH and **(c)** precipitation anomalies and zonal and meridional winds anomaly at 1000 hPa (vectors; unit: m/s) induced by ENSO, respectively. Panels **(b)** and **(d)** are the same as panels **(a)** and **(c)**, respectively, but for IOD effect. The units for SSHA, precipitation anomaly, and wind are cm, mm/day, and m/s, respectively.

5. The decadal shift of IOD impact on EIO upwelling

Figure 5 is the time-varying coefficient b_1 based on BDLM. Interestingly, we found that in the EIO, the IOD impact reversed before and after 1985 (**Figure 5b**). Previous studies also found that climate shift exists before and after 1985[1,56,57]. Dong and McPhaden[56] found that the relationship between SST in the Indian and Pacific Ocean underwent a dramatic transformation beginning around 1985. More specifically, prior to 1985, SST variations associated with the Indian Ocean basin mode (IOB) and the interdecadal Pacific oscillation (IPO) were positively correlated, whereas afterward they were much less clearly synchronized. Zhang et al.[57] further showed that the subtropical Indian Ocean dipole has been weakening in recent decades and Ningaloo Nino has been strengthening. In order to see the related processes that may cause this decadal shift in impacts, we estimated regressions of SSTA, precipitation and wind stress onto IOD index for the period of 1958–1984 and 1985–2016 (**Figure 6**). Strong and weak easterlies appear along the Indian Ocean's eastern coast, and are accompanied by differences in atmospheric circulations over the western Pacific and Indian subcontinent as well as precipitation patterns in the Indian Ocean (more negative in the eastern Indian Ocean before 1985 than afterward). The Pacific Ocean temperature also shows different patterns before and after 1985, namely a basin warming before 1985 compared to a central Pacific El Niño like pattern afterwards. Even though the zonal SST contrast in the equatorial Indian Ocean is assumed to be unity, the relatively stronger easterlies along the coastal area of EIO before 1985s drives a relatively stronger upwelling as shown in **Figure 6b**.

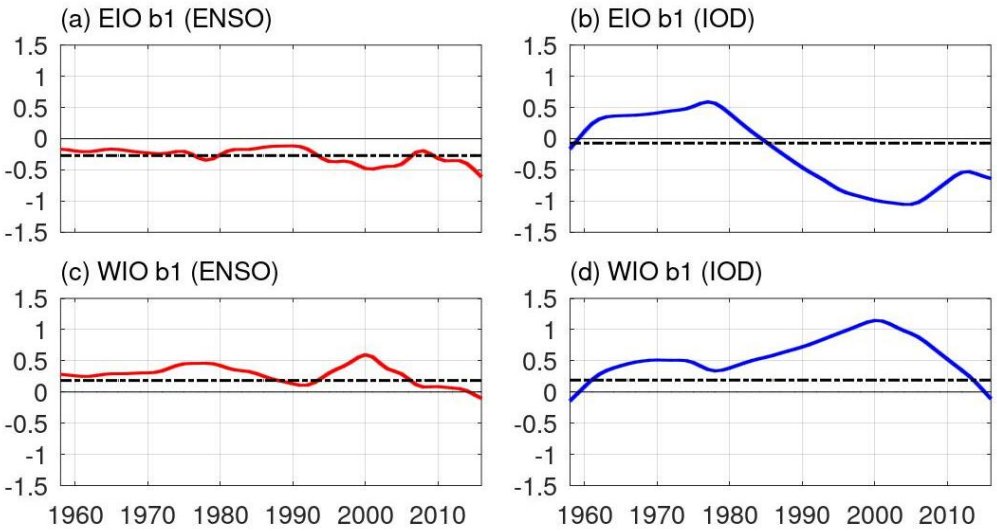

Figure 5. Time series of regression coefficient $b_1(t)$ based on BDLM for ENSO contribution in the **(a)** EIO and **(c)** WIO boxed region. **(b)**, **(d)** are the same as **(a)**, **(c)**, but for IOD impact. The horizontal dashed-dotted line in each panel is the constant SLM coefficient (b_1).

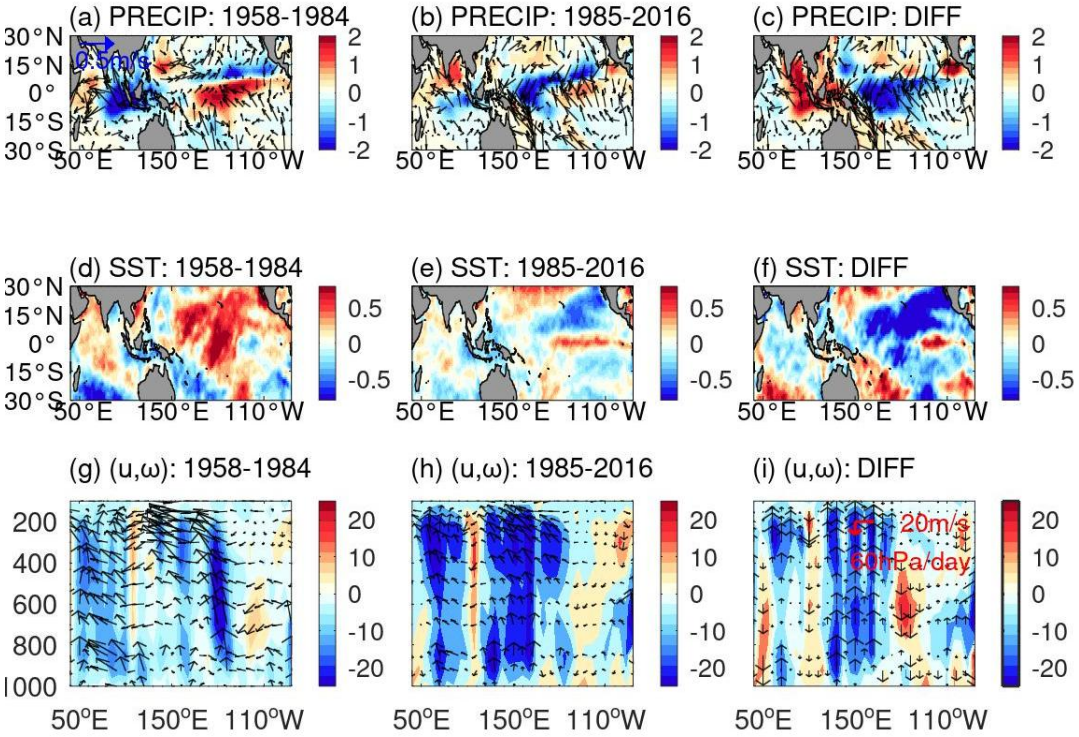

Figure6. Regression onto SON DMI (7-year filter) for precipitation (color shading; unit: mm/day) and zonal and meridional winds anomaly at 1000 hPa (vectors; unit: m/s) during the periods **(a)** 1958–1984 and **(b)** 1985–2016. **(c)** Differences of these two periods (i.e., panel **(b)** minus panel **(a)**). **(d)**–**(f)** are the same as **(a)**–**(c)**, but for SST (color shading; unit: ℃). **(g)**–**(i)** are the same as **(a)**–**(c)**, but for the zonal and vertical winds (vectors; unit: m/s and hPa/day, respectively) along the equatorial Indo-Pacific Ocean. Shades represent vertical wind velocity.

As discussed in our recent work[58], the background ocean temperature change may also have an important impact on the decadal shift impact of IOD on EIO upwelling. The difference in upper 200 m ocean temperature along the equatorial Indian-Pacific Ocean, and the Walker circulation cell before and after 1985 are shown in **Figure 7**. We can see that after 1985, there was a strong warming tendency in the surface layer

of the Indo-Pacific Oceans (**Figure 7b**) together with the changes in Indo-Pacific Walker circulation (**Figure 7a**). Also note here, that a strong vertical temperature gradient appears in the eastern Indian Ocean to accompany this ocean warming. As a result, the coastal wind in the eastern Indian Ocean induces the IOD signal more effectively in EIO. The optimized values of the coefficient b_1 represent changes in the efficiency in forming the IOD signal in EIO as an ocean response to the surface wind stress forcing aloft, corresponding to changes in the background states of the Indian Ocean.

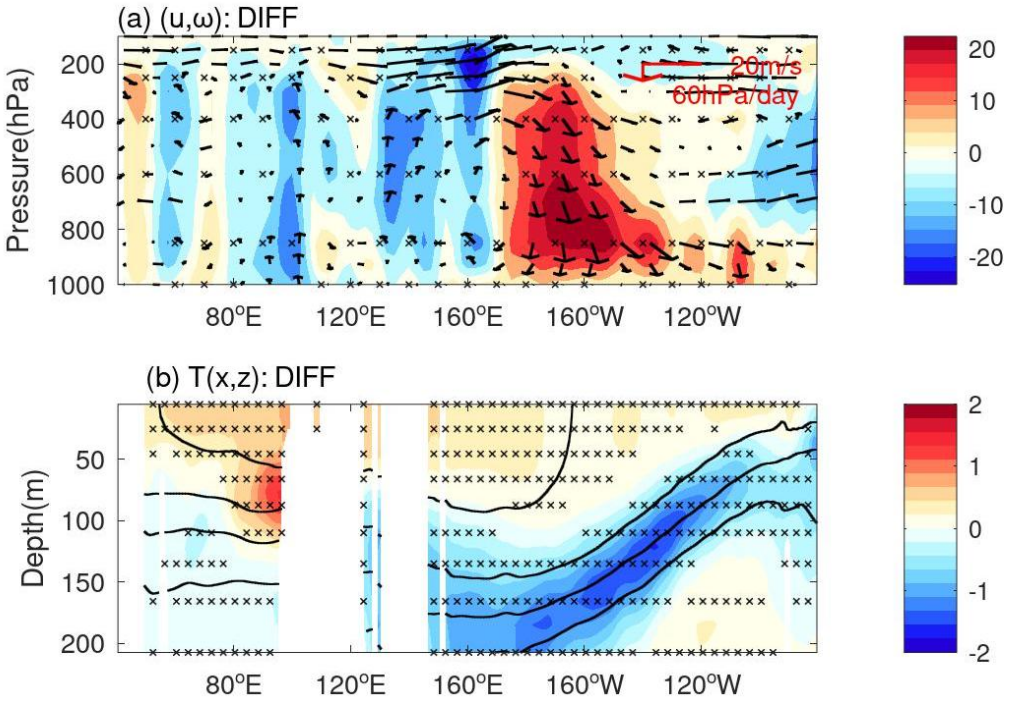

Figure 7. (a) The difference of equatorial vertical wind velocity (shade, hPa/day), and zonal (m/s) and vertical wind velocity (vectors) along the equatorial Indian Pacific Ocean before and after 1985 (i.e., values after 1985 minus those before 1985). **(b)** The difference of ocean temperature before and after 1985 (shade, ℃), and the climatology (bold curves, ℃). Cross marks represent the significant differences at a 95% confidence limit. The missing data between 80° E and 160° E in **(b)** is caused by continent that has no temperature data available.

Pacific Decadal Oscillation (PDO) is one of the major decadal variabilities on earth. What's the link between PDO and the decadal shift impact of IOD on the upwelling in EIO? A possible process is that during the positive PDO phase, the IOD has a stronger impact on EIO upwelling; in contrast, during the negative PDO phases (before 1976 and after 2002), the IOD has a weaker impact on upwelling in the EIO. Further studies are required to explore more details.

6. Conclusion and discussion

By combining the observational data since 1958 and statistical models, our results suggest that there are two high variabilities in the EIO and WIO and the upwellings are positively correlated in these two regions (**Figures 1** and **2**). The SLM and BDLM analysis suggest that overall BDLM simulation is better than the SLM result (**Figure 4**) and in both WIO and EIO boxed regions, IOD is more important than ENSO impact. We also found that the optimized values in the regression coefficients contribute to representing the effects of decadal variations of the background climate states that can modulate the strength of the Indian Ocean upwelling. For example, there is a decadal shift of IOD impact before and after 1985s for the EIO upwelling (**Figure 5**). This is mainly caused by the shift of wind stress forcing along the eastern coast in magnitudes, corresponding to the changes in sensitivity of the ocean response to atmospheric forcing in relation to the

strength of upper ocean stratification (**Figures 6** and **7**). Our advanced statistical model (BDLM) has estimated the time-varying impact of climate modes on Indian Ocean upwellings, which is more realistic and can be used for future studies. Even though the BDLM shows significant advantages over the SLM in estimating the climate modes' impacts, the simultaneous relationships between the climate mode indices and upwelling indicators cannot properly capture the contribution of oceanic waves, careful studies are needed to evaluate the contribution of wave processes.

Furthermore, some questions are still unclear, for instance, the relationship between the decadal shift of IOD impact and PDO. These can be a topic for future study. In addition, the upwelling as a response of the ocean to wind stress forcing can represent feedback to wind stress forcing. However, this contribution is not well represented in our research, future studies are required to explore more details about the ocean-atmosphere coupled processes. Direct verification of coupled climate processes modulating the ocean upwelling is also an interesting research question for future works. Nevertheless, we have built on the study of Zhang and Han [2], which mainly focused on the ocean upwelling on interannual time scales, by showing some important processes that primarily affect the impact of climate modes on decadal timescales. Our results also suggest that the changing atmosphere-ocean state in the climate models towards precise simulations of the impact of climate modes on the Indian Ocean upwelling.

Acknowledgments

We gratefully acknowledge funding from the Japan Society for the Promotion of Science (JSPS) KAKENHI (grant JP19H05703) and the discussions with Mochizuki Takashi and Chenxi Zhai for their significant improvements to our work. Thanks are also due to Weiqing Han for her support in performing the linear model estimations.

Conflict of interest

The author declares no conflict of interest.

Abbreviations

AVISO	Archiving, Validation, and Interpretation of Satellite Oceanography
BDLM	Bayesian Dynamic Linear Model
D20	Depth of 20 Degree Isotherm
DLM	Dynamic Linear Model
DMI	Dipole Mode Index
ECMWF	European Centre for Medium-Range Weather Forecasts
EIO	Eastern Indian Ocean
ENSO	El Niño and Southern Oscillation
HadISST	Hadley Centre Sea Ice and Sea Surface Temperature
IO	Indian Ocean
IOB	Indian Ocean Basin Mode
IOD	Indian Ocean Dipole
IPO	Interdecadal Pacific Oscillation
NCEP	National Centers for Environmental Prediction
NOAA	National Oceanic and Atmospheric Administration
ORAS4	Ocean Reanalysis System 4
PDO	Pacific Decadal Oscillation
SCTR	Seychelles–Chagos Thermocline Ridge
SLA	Sea Level Anomaly
SLM	Static Linear Regression Model
SSH	Sea Surface Height
SSHA	SSH Anomaly
SST	Sea Surface Temperature
SSTA	Sea Surface Temperature Anomaly
STD	Standard Deviation

WIO	Western Indian Ocean
WOA13	World Ocean Atlas 2013

References

1. Han W, Vialard J, McPhaden MJ, et al. Indian Ocean decadal variability: A review. *Bulletin of the American Meteorological Society* 2014; 95: 1679–1703. doi: 10.1175/BAMS-D-13-00028.1
2. Zhang X, Han W. Effects of climate modes on interannual variability of upwelling in the tropical Indian Ocean. *Journal of Climate* 2020; 33(4): 1547–1573. doi: 10.1175/JCLI-D-19-0386.1
3. Chen G, Han W, Li Y, Wang D. Interannual variability of eastern Indian Ocean upwelling: Local versus remote forcing. *Journal of Physical Oceanography* 2016; 46(3): 789–807. doi: 10.1175/JPO-D-15-0117.1
4. McCreary Jr. JP, Kundu PK, Molinari RL. A numerical investigation of dynamics, thermodynamics and mixed-layer processes in the Indian Ocean. *Progress in Oceanography* 1993; 31(3): 181–244. doi: 10.1016/0079-6611(93)90002-U
5. Murtugudde RG, Signorini SR, Christian JR, et al. Ocean color variability of the tropical Indo-Pacific basin observed by SeaWiFS during 1997–1998. *Journal of Geophysical Research* 1999; 104(C8): 18351–18366.
6. Hermes JC, Reason CJC. Annual cycle of the South Indian Ocean (Seychelles-Chagos) thermocline ridge in a regional ocean model. *Journal of Geophysical: Oceans* 2008; 113(C4): C04035. doi: 10.1029/2007JC004363
7. Yokoi T, Tozuka T, Yamagata T. Seasonal variation of the Seychelles Dome. *Journal of Climate* 2008; 21(15): 3740–3754. doi: 10.1175/2008JCLI1975
8. Yokoi T, Tozuka T, Yamagata T. Seasonal variation of the Seychelles Dome simulated in the CMIP3 models. *Journal of Physical Oceanogrphy* 2009; 39(2): 449–457. doi: 10.1175/2008JPO3914.1
9. Susanto RD, Gordon AL, Zheng Q. Upwelling along the coasts of Java and Sumatra and its relation to ENSO. *Geophysical Research Letters* 2001; 28(8): 1599–1602.
10. Schott FA, Xie SP, McCreary JP. Indian Ocean circulation and climate variability. *Reviews of Geophysics* 2009; 47(1): RG1002. doi: 10.1029/2007RG000245
11. Tozuka T, Yokoi T, Yamagata T. A modeling study of interannual variations of the Seychelles Dome. *Journal of Geophysical Research* 2010; 115: C04005. doi: 10.1029/2009JC005547
12. Trenary L, Han W. Intraseasonal to interannual variability of South Indian Ocean sea level and thermocline: Remote versus local forcing. *Journal of Physical Oceanography* 2012; 42(4): 602–627. doi: 10.1175/JPO-D-11-084.1
13. Woodberry KE, Luther ME, O'Brien JJ. The wind-driven seasonal circulation in the southern tropical Indian Ocean. *Journal of Geophysical Research* 1989; 94(C12): 17985–18002. doi:10.1029/JC094Ic12P17985
14. Périgaud C, Delecluse P. Annual sea level variations in the southern tropical Indian Ocean from Geosat and shallow-water simulations. *Journal of Geophysical Research* 1992; 97(C12): 20169–20178. doi: 10.1029/92JC01961
15. Périgaud C, Delecluse P. Interannual sea level variations in the tropical Indian Ocean from Geosat and shallow water simulations. *Journal of Physical Oceanography* 1993; 23(9): 1916–1934. doi: 10.1175/1520-0485(1993)023<1916:ISLVIT>2.0.CO;2
16. Fu LL, Smith RD. Global ocean circulation from satellite altimetry and high-resolution computer simulation. *Bulletin of the American Meteorological Society* 1996; 77(11): 2625–2636.
17. Masumoto Y, Meyers G. Forced Rossby waves in the southern tropical Indian Ocean. *Journal of Geophysical Research* 1998; 103(C12): 27589–27602. doi: 10.1029/98JC02546
18. Yang J, Yu L, Koblinsky CJ, Adamec D. Dynamics of the seasonal variations in the Indian Ocean from TOPEX/POSEIDON sea surface height and an ocean model. *Geophysical Research Letters* 1998; 25(11): 1915–1918. doi: 10.1029/98GL01401
19. Chambers DP, Tapley BD, Stewart RH. Anomalous warming in the Indian Ocean coincident with El Niño. *Journal of Geophysical: Oceans* 1999; 104(C2): 3035–3047. doi: 10.1029/1998JC900085
20. White WB. Evidence for coupled Rossby waves in the annual cycle of the Indo-Pacific Ocean. *Journal of Physical Oceanography* 2001; 31(10): 2944–2957. doi: 10.1175/1520-0485(2001)031<2944:EFCRWI>2.0.CO;2
21. Birol F, Rosemary M. Source of the baroclinic waves in the southeast Indian Ocean. *Journal of Geophysical Research* 2001; 106(C5): 9145–9160 doi: 10.1029/2000JC900044
22. Wang L, Koblinsky CJ, Howden S. Annual Rossby wave in the Southern Indian Ocean: Why does it "appear" to break down in the middle ocean? *Journal of Physical Oceanography* 2001; 31: 54–74.
23. Jury MR, Huang B. The Rossby wave as a key mechanism of Indian Ocean climate variability. *Deep Sea Research Part I: Oceanographic Research Papers* 2004; 51(12): 2123–2136. doi: 10.1016/j.dsr.2004.06.005
24. Baquero-Bernal A, Latif M. Wind-driven oceanic Rossby waves in the Tropical South Indian Ocean with and without an active ENSO. *Journal of Physical Oceanography* 2005; 35(5): 729–746. doi: 10.1175/JPO2723.1
25. Rao SA, Behera SK. Subsurface influence on SST in the tropical Indian Ocean: Structure and interannual variability. *Dynamics of Atmospheres and Oceans* 2005; 39(1–2): 103–139. doi: 10.1016/j.dynatmoce.2004.10.014

26. Zhuang W, Feng M, Du Y, et al. Low-frequency sea level variability in the southern Indian Ocean and its impacts on the oceanic meridional transports. *Journal of Geophysical Research Oceans* 2013; 118(3): 1302–1315. doi: 10.1002/jgrc.20129
27. Potemra JT. Contribution of equatorial Pacific winds to southern tropical Indian Ocean Rossby waves. *Journal of Geophysical Research* 2001; 106(C2): 2407–2422. doi: 10.1029/1999JC000031
28. Deepa JS, Gnanaseelan C, Kakatkar R, et al. The interannual sea level variability in the Indian Ocean as simulated by an Ocean General Circulation Model. *International Journal of Climatology* 2018; 38(3): 1132–1144. doi: 10.1002/joc.5228
29. Hu S, ZhangY, Feng M, et al. Interannual to decadal variability of upper-ocean salinity in the Southern Indian Ocean and the role of the Indonesian throughflow. *Journal of Climate* 2019; 32(19): 6403–6421. doi: 10.1175/JCLI-D-19-0056.1
30. Huang B, Kinter III JL. Interannual variability in the tropical Indian Ocean. *Journal of Geophysical Research* 2002; 107(C11): 3199. doi: 10.1029/2001JC001278
31. Xie SP, Annamalai H, Schott FA, McCreary JP. Structure and mechanisms of South Indian Ocean climate variability. *Journal of Climate* 2002; 15(8): 864–878. doi: 10.1175/1520-0442(2002)015<0864:SAMOSI>2.0.CO;2
32. Yu W, Xiang B, Liu L, Liu N. Understanding the origins of interannual thermocline variations in the tropical Indian Ocean. *Geophysical Research Letters* 2005; 32(24): L24706. doi: 10.1029/2005GL024327
33. Gnanaseelan C, Vaid BH. Interannual variability in the Biannual Rossby waves in the tropical Indian Ocean and its relation to Indian Ocean Dipole and El Niño forcing. *Ocean Dynamics* 2010; 60(1): 27–40. doi: 10.1007/s10236-009-0236-z
34. Murtugudde R, McCreary JP, Busalacchi AJ. Oceanic processes associated with anomalous events in the Indian Ocean with relevance to 1997–1998. *Journal of Geophysical Research Atmospheres* 2000; 105(C2): 3295–3306. doi: 10.1029/1999JC900294
35. Han W, Webster PJ. Forcing mechanisms of sea-level interannual variability in the Bay of Bengal. *Journal of Physical Oceanography* 2002; 32(1): 216–239. doi: 10.1175/1520-0485(2002)032<0216:FMOSLI>2.0.CO;2
36. Shinoda T, Hendon H, Alexander MA. Surface and subsurface dipole variability in the Indian Ocean and its relation with ENSO. *Deep Sea Research Part I* 2004; 51(5): 619–635. doi: 10.1016/j.dsr.2004.01.005
37. Balmaseda MA, Trenberth KE, Källén E. Distinctive climate signals in reanalysis of global ocean heat content. *Geophysical Research Letters* 2013; 40(9): 1754–1759. doi: 10.1002/grl.50382
38. Rayner NA, Parker DE, Horton EB, et al. Global analyses of sea surface temperature, sea ice, and night marine air temperature since the late nineteenth century. *Journal of Geophysical Research* 2003; 108(D14): 4407. doi: 10.1029/2002JD002670
39. Levitus S, Antonov JI, Boyer TP, et al. World ocean heat content and thermosteric sea level change (0–2000 m), 1955–2010. *Geophysical Research Letters* 2012; 39(10): L10603. doi:10.1029/2012gl051106
40. Kalnay E, Kanamitsu M, Kistler R, et al. The NCEP/NCAR 40-year reanalysis project. *Bulletin of the American Meteorological Society* 1996; 7(3): 7437–471. doi: 10.1175/1520-0477(1996)077<0437:TNYRP >2.0.CO;2
41. Xie P, Arkin PA. Analyses of global monthly precipitation using gauge observations, satellite estimates, and numerical model predictions. *Journal of Climate* 1996; 9(4): 840–858. doi: 10.1175/1520-0442(1996)009<0840:AOGMPU>2.0.CO;2
42. Xie P, Arkin PA. Global precipitation: A 17-year monthly analysis based on gauge observations, satellite estimates, and numerical model outputs. *Bulletin of the American Meteorological Society* 1997; 78(11): 2539–2558. doi: 10.1175/1520-0477(1997)078<2539:GPAYMA>2.0.CO;2
43. Saji NH, Goswami BN, Vinayachandran PN, Yamagata T. A dipole mode in the tropical Indian Ocean. *Nature* 1999; 401(6751): 360–363. doi: 10.1038/43854.
44. Xie SP, Du Y, Huang G, Zheng XT, et al. Decadal shift in El Niño influences on Indo-western Pacific and East Asian climate in the 1970s. *Journal of Climate* 2010; 23(12): 3352–3368. doi: 10.1175/2010JCLI3429.1
45. Annamalai H, Liu p, Xie SP. Southwest Indian Ocean SST variability: Its local effect and remote influence on Asian monsoons. *Journal of Climate* 2005; 18(20): 4150–4167. doi: 10.1175/JCLI3533.1
46. Kumar KK, Rajagopalan B, Cane MA. On the weakening relationship between the Indian monsoon and ENSO. *Science* 1999; 284(5423): 2156–2159. doi: 10.1126/science.284.5423.2156
47. Ashok K, Chan WL, Motoi T, Yamagata T. Decadal variability of the Indian Ocean Dipole. *Geophysical Research Letters* 2004; 31(24): 207. doi: 10.1029/2004GL021345
48. Krishnaswamy J, Vaidyanathan S, Rajagopalan B, et al. Non-stationary and non-linear influence of ENSO and Indian Ocean Dipole on the variability of Indian monsoon rainfall and extreme rain events. *Climate Dynamics* 2015; 45: 175–184. doi: 10.1007/s00382-014-2288-0
49. Han W, Meehl GA, Stammer D, et al. Spatial patterns of sea level variability associated with natural internal climate modes. *Surveys in Geophysics* 2017; 38(1): 217–250. doi: 10.1007/s10712-016-9386-y

50. Han W, Stammer D, Meehl GA, et al. Multi-decadal trend and decadal variability of the regional sea level over the Indian Ocean since the 1960s: Roles of climate modes and external forcing. *Climate* 2018; 6(2): 341–356. doi: 10.3390/cli6020051
51. Izumo T, Vialard J, Lengaigne M, et al. Influence of the state of the Indian Ocean Dipole on the following year's El Niño. *Nature Geoscience* 2010; 3: 168–172. doi: 10.1038/Ngeo760
52. Petris G, Petrone S, Campagnoli P. *Dynamic Linear Models with R*. Springer; 2009. pp. 31–84.
53. Petris G. Dlm: Bayesian and likelihood analysis of dynamic linear models. R package version 1.1-6; 2022. Available online: https://cran.r-project.org/web/packages/dlm/dlm.pdf (accessed on 28 August 2023).
54. R Development Core Team. R: A language and environment for statistical computing. R Foundation for Statistical Computing; 2016.
55. Zhang X, Mochizuki T. Sea surface height fluctuations relevant to Indian summer monsoon over the northwestern Indian Ocean. *Frontiers in Climate* 2022; 4: 1008776. doi: 10.3389/fclim.2022.1008776
56. Dong L, McPhaden MJ. Why has the relationship between Indian and Pacific Ocean decadal variability changed in recent decades? *Journal of Climate* 2017; 30(6): 1971–1983. doi: 10.1175/JCLI-D-16-0313.1
57. Zhang L, Han W, Karnauskas KB, et al. Eastward shift of interannual climate variability in the South Indian Ocean since 1950. *Journal of Climate* 2022; 35(2): 561–575. doi: 10.1175/JCLI-D-21-0356.1
58. Zhang X, Mochizuki T. Decadal modulation of ENSO and IOD impacts on the Indian Ocean upwelling. *Frontier in Earth Science* 2023; 11: 1212421. doi: 10.3389/feart.2023.1212421